Inorganic Chemistry

Article

pubs.acs.org/IC

$Ni_3Cl_{2.1}(OH)_{3.9}\cdot 4H_2O$, the Ni Analogue to $Mg_3Cl_2(OH)_4\cdot 4H_2O$

Sebastian Bette,[†] Robert E. Dinnebier,[‡] and Daniela Freyer*[,†]

[†]TU Bergakademie Freiberg, Institute of Inorganic Chemistry, Leipziger Strasse 29, 09596 Freiberg, Germany

[‡]Max Planck Institute for Solid State Research, Heisenbergstrasse 1, 70569 Stuttgart, Germany

Supporting Information

ABSTRACT: For the first time a basic transition-metal hydrate, $Ni_3Cl_{2.1}(OH)_{3.9}\cdot 4H_2O$, is found to be isostructural to a main-group metal phase, $Mg_3Cl_{2.0}(OH)_{4.0}\cdot 4H_2O$. The Ni phase was found as crystalline solid in the course of investigations into the formation of basic nickel(II) chloride phases at 25 and 40 °C in alkaline, concentrated nickel(II) chloride solutions. $Ni_3Cl_{2.1}(OH)_{3.9}\cdot 4H_2O$ was characterized by thermal analysis, IR spectroscopy, scanning electron microscopy, and X-ray powder diffraction. The crystal structure was determined from high-resolution laboratory X-ray powder diffraction data. $Ni_3Cl_{2.1}(OH)_{3.9}\cdot 4H_2O$ crystallizes in space group $C2/m$ (12) with $Z = 2$, $a = 14.9575(4)$ Å, $b = 3.1413(1)$ Å, $c = 10.4818(5)$ Å, $\beta = 101.482(1)°$, and $V = 482.50(3)$ Å^3. The main building unit of the structure is an infinite triple chain of edge-linked distorted NiO_6 octahedra. These chains are separated by interstitial one-dimensional zigzag chains of disordered Cl^- ions and H_2O molecules. The crystal structures of $Ni_3Cl_{2.1}(OH)_{3.9}\cdot 4H_2O$ and the isostructural magnesium salt hydrate $Mg_3Cl_2(OH)_4\cdot 4H_2O$ (2−1−4 phase) are compared in detail.

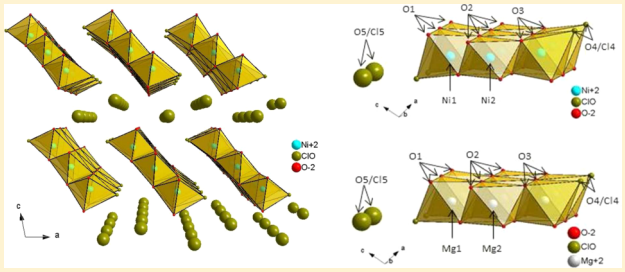

INTRODUCTION

The formation conditions, existence, properties, and crystal structures of basic metal(II) salts have been subject to numerous investigations for nearly 150 years. The main focus is on the system $Mg(OH)_2$−$MgCl_2$−H_2O as it represents the scientific base for the production of magnesia cement (Sorel cement[1]). Different basic magnesium chloride hydrates with the composition of $xMg(OH)_2\cdot yMgCl_2\cdot zH_2O$, where x−y−z = 3−1−8, 5−1−8, 9−1−4, 2−1−4, 2−1−2, and 3−1−0, were characterized,[2−23] and their crystal structures were determined.[24−28]

A comparison of the chemical properties, the ionic radii,[29] and the coordination in inorganic salts reveals some analogies between Mg^{2+} and Ni^{2+} ions. Their hydroxides crystallize in the same brucite-type lattice,[30] the crystal structures of the magnesium and nickel(II) chloride hydrates ($MCl_2\cdot xH_2O$, x = 2, 4, 6,)[31−33] show comparable motives,[34−36] and Feitknecht[6] synthesized a basic nickel(II) chloride (β-$Ni_2Cl(OH)_3$), which he expected to crystallize in an atacamite-type lattice, analogous to β-$Mg_2Cl(OH)_3$ (3−1−0 phase).

Like magnesium, nickel forms basic metal(II) salt hydrates, so the structure of a basic nickel(II) sulfate hydrate $Ni_3(OH)_2(SO_4)_2(H_2O)_2$ is already known.[37] Investigations to the phase formation of basic nickel(II) chloride hydrates in the system $Ni(OH)_2$−$NiCl_2$−H_2O were done by Feitknecht[38] in the way of systematic precipitation reactions of sodium hydroxide with nickel(II) chloride solutions of different concentrations from 25 to 100 °C. The authors found three different basic nickel(II) chloride hydrates distinguished by X-ray powder diffraction: the given compositions $xNi(OH)_2$−$yNiCl_2$−zH_2O were (6−7)−1−z obtained with 1.1 m $NiCl_2$ solution, (3−4)−1−z with 1.7 m $NiCl_2$ solution, and 2−1(3−4) obtained with 4.7 m $NiCl_2$ solution. Feitknecht also stated that the crystallization process of the phases is very slow and that all basic nickel(II) chloride hydrates he received were of poor crystallinity. All attempts to remove adherent mother solution by washing with deionized water caused the decomposition of the phases. So, Feitknecht was able neither to obtain pure phases nor to estimate the exact phase compositions. The nearly (6−7)−1−z and (3−4)−1−z stoichiometries according to Feitknecht[38] were reproduced by Makovskaya[39] for the solid phase obtained by precipitation of sodium hydroxide with diluted and higher concentrated nickel chloride solutions at room temperature. Makovskaya also failed in the exact stoichiometry determination of these phases. Other authors[40−42] received just as poorly characterized compounds of a nearly similar composition (6−7)−1−z at ambient conditions by incomplete precipitation of dilute nickel(II) chloride solution with ammonia,[40] by oxidation of magnesium metal in nickel(II) chloride solutions,[41] and by electrolysis of dilute nickel chloride solution.[42]

To get more definite structural information about basic nickel(II) chloride phases, we synthesized and characterized the basic nickel(II) chloride hydrate $Ni_3Cl_{2.1}(OH)_{3.9}\cdot 4H_2O$ (1.95−1.05−4 phase), obtained during systematic investigations in the system $Ni(OH)_2$−$NiCl_2$−H_2O at 25 and 40 °C. Because of the slow crystallization of initially formed amorphous solids no single crystals were available. To determine the crystal structure, high-resolution laboratory X-ray powder diffraction experiments were carried out. The present work focuses on the

Received: December 4, 2013
Published: April 22, 2014

   dx.doi.org/10.1021/ic500251x | *Inorg. Chem.* 2014, 53, 4316−4324

chemical composition, spectroscopic properties, thermal behavior, and structural characterization of the $Ni_3Cl_{2.1}(OH)_{3.9}·4H_2O$ phase in comparison to the related basic magnesium chloride hydrate $Mg_3Cl_2(OH)_4·4H_2O$.

EXPERIMENTAL SECTION

Phase Formation, Isolation, and Characterization. To reproduce the experiments carried out by Feitknecht,[38] 3.5 g of solid sodium hydroxide pallets (Sigma-Aldrich, p.a.) were added to 80 g of a 1.1, 1.7, and 4.7 *m* nickel chloride solution (dissolution of nickel chloride hexahydrate (VWR, p.a.) in deionized water) at room temperature. The suspension was homogenized by stirring for 1.5 h. Afterward the mixture was transferred to a sealed polypropylene vessel and tempered in a water bath at 40 °C for three months. The suspensions were shaken three times each week. For further investigations the solid phases were filtered from the mother liquor and washed several times with cold (T < 5 °C) deionized water. Finally the solid phase was washed with cold (T < 5 °C) ethanol to remove adherent water and dried at room temperature. The phase purity was controlled by standard laboratory X-ray powder diffraction (D8 Bruker). Out of three solid phases only the one that was prepared from the most concentrated (4.7 *m*) nickel chloride solution showed an X-ray powder pattern; the other two were amorphous. The thermal analysis was carried out using a TG/DTA 22 of Seiko instruments (reference substance: Al_2O_3, open platinum crucible, argon flow 300 mL min^{-1}, heating rate 2 K min^{-1}). The residue after heating up to 375 and 600 °C was examined by X-ray powder diffraction. IR spectra were recorded from KBr blanks using a Fourier transform (FT) IR spectrometer Nicolet 380X (Thermo Electron Company) with DLaTGS-Detector. Scanning electron microscopy (SEM) pictures were taken with a LEO 1530 Gemini (20 kV accelerating voltage) after the sample was coated with gold.

The chemical composition of the solid phase was determined as $Ni_3Cl_{2.1}(OH)_{3.9}·4\ H_2O$ by chemical analysis of the Ni^{2+}-, Cl^--, and OH^--content. Therefore, the sample was dissolved in 1 M nitric acid. The Ni^{2+} content was determined by complexometric titration with 0.05 M sodium ethylendiaminetetraacetate (Na-EDTA) in a NH_3/NH_4Cl buffered solution using Murexide as indicator, and the Cl^- content was determined by titration with 0.1 M $AgNO_3$ at pH 8−9 using K_2CrO_4 as indicator. The OH^--content was determined by potentiometric acid back-titration (therefore a sample of the solid was dissolved in 1.0 M HCl) with 0.1 M NaOH and a pH glass electrode from Ross Orion 8103 BN (Thermo Scientific).[43] The amount of water was calculated both out of the mass balance and the thermal analysis.

To screen the phase formation of basic nickel chloride hydrates in the system $Ni(OH)_2$−$NiCl_2$−H_2O, 2 g of nickel hydroxide (ABCR, p.a.) was added to 40 g of 0.3, 0.5, 1.0, 1.5, 2.0, 3.5, and 5.0 *m* nickel chloride solutions. The mixtures were tempered in sealed polypropylene vessels in a water bath at 25 and 40 °C for three months and shaken three times each week. After filtration the compositions of the solid phases as well as of the solutions (amounts of Ni^{2+}, Cl^-, and OH^-) were determined by chemical analysis (see above). X-ray powder diffraction patterns were recorded for all solid phases.

Laboratory Powder Diffraction. The X-ray powder diffraction pattern of $Ni_3Cl_{2.1}(OH)_{3.9}·4\ H_2O$ was collected at room temperature on a laboratory powder diffractometer (Stadi P-Diffraktometer, Stoe, Mo $K_{\alpha 1}$ radiation from primary Ge(111) Johannson-type monochromator, Mythen 1 K detector, Dectris) in Debye−Scherrer geometry. The sample was sealed in a 0.5 mm diameter borosilicate glass capillary (Hilgenberg glass No. 14), which was spun during the measurement. Data were taken in increments of 0.012° 2θ using a scanning speed of 15 s per step from 2° to 60° 2θ (20 h total). Further experimental details are given in Table 2.

The program TOPAS 4.2[44] was used to determine and refine the crystal structure. Indexing of the phase was carried out by an iterative use of singular value decomposition,[45] leading to a C-centered monoclinic unit cell with lattice parameters given in Table 5. The most probable space group was determined as $C2$ (5) or $C2/m$ (12) from the observed extinction rules. Considering both the volume of the unit cell (Table 5), the number of non-H atoms ($Ni_3(OH)_{3.9}Cl_{2.1}·(H_2O)_4$ = 3 × Ni, 2.1 × Cl, 7.9 × O, = 13 non-H atoms) and the fact that each of these atoms takes up about 18 Å^3, Z was determined to be 2. The peak profile and the precise lattice parameters were determined by Le Bail fits[46] applying the fundamental parameter (FP) approach of TOPAS.[47] The background was modeled by employing Chebychev polynomials. The amorphous hump caused by the glass capillary was modeled by using a very broad Lorentzian-shaped peak. To account for the anisotropic peak broadening induced by microstrain, symmetry-adapted spherical harmonics of the fourth order were successfully applied. The refinement converged quickly.

Table 1. Crystallographic and Rietveld Refinement Data for $Ni_3Cl_{2.1}(OH)_{3.9}·4H_2O$ at Ambient Conditions

compound name	1.95−1.05−4 phase
molecular formula	$Ni_3Cl_{2.1}(OH)_{3.9}·4H_2O$
sum formula	$Ni_3O_{7.9}Cl_{2.1}H_{11.9}$
molecular weight (g/mol)	388.909
space group	$C2/m$
Z	2
a /Å	14.9575(4)
b /Å	3.1413(1)
c /Å	10.4818(5)
β /deg	101.482(1)
V /Å^3	482.49(3)
ρ_{calc} /g cm^{-3}	2.67
wavelength /Å	0.709 30
R-exp /%[a]	0.23
R-p /%[a]	2.15
R-wp /%[a]	2.76
R-F^2 /%[a]	0.73
starting angle (deg 2θ)	2.0
final angle (deg 2θ)	60.0
step width (deg 2θ)	0.012
time/scan (h)	20
no. of variables	56

[a] R-exp, R-p, R-wp, and R-F^2 as defined in TOPAS (Bruker AXS).[49]

The crystal structure of $Ni_3Cl_{2.1}(OH)_{3.9}·4H_2O$ was solved by applying the global optimization method of simulated annealing (SA) in real space as it is implemented in TOPAS.[48] At the beginning a set of individual atoms (3 × Ni^{2+}, 2 × Cl^-, 8 × O^{2-}) was introduced into the SA process. Atoms located on identical positions and occupying special positions were identified by using a merging radius of 0.7 Å. After 2 h the positions of all atoms were found, and $C2/m$ was confirmed as the correct space group. The process was carried out several times to confirm the reproducibility of the result. Falsely assigned atom types were detected and corrected by visual inspection. Occupational disorder at the O(4) and Cl(5) site was identified by checking the Fourier map. So an additional Cl^- ion [Cl(4)] was introduced constraining its atomic coordinates to those of O(4). A variable was used to refine the occupancies of O(4) and Cl(4), constraining the sum of both values to 1. The same procedure was carried out at the site Cl(5), introducing an additional O^{2-} atom [O(5)]. A global variable was introduced to constrain the occupancies of the occupationally disordered atoms to the phase composition derived from both chemical and thermal analysis. For the final Rietveld refinement, all profile and lattice parameters were released iteratively, and all atomic positions were subjected to free unconstrained refinement (Figure 1). Final agreement factors (R values) are listed in Table 1. The atomic coordinates are given in Table 2, and selected bond distances and angles can be found in Table 3. The crystallographic data were deposited at ICSD and CSD-No. 427116.

dx.doi.org/10.1021/ic500251x | Inorg. Chem. 2014, 53, 4316−4324

Table 2. Atomic Coordinates of $Ni_3Cl_{2.1}(OH)_{3.9}\cdot 4H_2O$ at Ambient Conditions

atom	Wyck.	site	S.O.F.	*x/a*	*y/b*	*z/c*	B, Å^2
Ni(1)	4*i*	*m*	1	0.1045(1)	0	0.3260(2)	1.07(5)
Ni(2)	2*d*	2/*m*	1	1/2	0	1/2	1.07(5)
O(1)	4*i*	*m*	1	0.3710(6)	0	0.5493(10)	1.17(12)
O(2)	4*i*	*m*	1	0.9756(6)	0	0.3641(9)	1.17(12)
O(3)	4*i*	*m*	1	0.5612(5)	0	0.1739(4)	1.17(12)
O(4)	4*i*	*m*	0.5148	0.7513(4)	0	0.7248(5)	4.16(20)
Cl(4)	4*i*	*m*	0.4852	0.7513(4)	0	0.7248(5)	4.16(20)
Cl(5)	4*i*	*m*	0.5548	0.3693(3)	0	0.0632(4)	4.16(20)
O(5)	4*i*	*m*	0.4452	0.3693(3)	0	0.0632(4)	4.16(20)

Table 3. Selected Bond Distances (Å) and Angles (deg) of $Ni_3Cl_{2.1}(OH)_{3.9}\cdot 4H_2O$ at Ambient Conditions

Ni(1)−O	2.030(6) (2x)
Ni(1)−O	2.046(9)
Ni(1)−O	2.239(6) (2x)
Ni(1)−O/Cl	2.324(6)
Ni(2)−O	2.103(6) (4x)
Ni(2)−O	2.095(1) (2x)
Ni(1)−Ni(2)	3.062(2)
O/Cl−O/Cl (min)	3.131(8)
O−O (min)	2.779(10)
O−Ni(1)−O	85.98(32)-95.23(30) 172.20(29), 178.08(20)
O−Ni(2)−O	82.91(30)-97.09(30) 180

RESULTS AND DISCUSSION

Phase Formation. *Precipitation of Basic Nickel(II) Chloride Hydrates Using NaOH.* Before systematic investigation to the formation of basic nickel(II) chloride phases in the system $Ni(OH)_2$−$NiCl_2$−H_2O were started, the experiments of Feitknecht[38] were reproduced. Accordingly, sodium hydroxide pellets were added to 1.1, 1.7, and 4.7 *m* nickel(II) chloride solutions. X-ray powder diffraction revealed that the precipitation products from 1.1 and 1.7 *m* nickel(II) chloride solutions were almost amorphous. There were only some weak and broad peaks in the diffraction patterns, which are also present in the diffraction data given by Feitknecht[38] for the basic nickel(II) chloride hydrates possessing the compositions of (6−7)−1−*z* and (3−4)−1−*z*. The solid phase obtained by using the most concentrated nickel(II) chloride solution (4.7 *m*) was well crystalline (very fine and short needles, Figure 2), and the diffraction pattern of this phase is almost equal to the data for Feitknecht's[38] 2−1−(3−4) phase. After chemical analysis a more detailed composition was determined and is given in Table 4. The crystal water content was obtained from mass balance of the chemical analysis as well as by thermal analysis with 4.2 ± 0.2 mol of water. In agreement with considerations out of structure solution and refinement (see below) exactly four molecules of crystal water should be contained.

Phase Formation in the System $Ni(OH)_2$−$NiCl_2$−H_2O at 25 and 40 °C. The systematic conversion of nickel(II) hydroxide with nickel(II) chloride solutions at 25 and 40 °C yielded either to $Ni(OH)_2$ or mixtures of $Ni(OH)_2$ and $Ni_3Cl_{2.1}(OH)_{3.9}\cdot 4H_2O$ (identified by the X-ray powder pattern of the phase $Ni_3Cl_{2.1}(OH)_{3.9}\cdot 4H_2O$ analyzed before) (Table 5). The composition of the corresponding liquid phase is plotted in Figure 3. The highest $NiCl_2$ solution concentration used for the experiments was 5.0 *m*. The curves end at the solubility of the pure hydrates of nickel chloride, at 25 °C the hexahydrate (5.06 *m*) $NiCl_2\cdot 6H_2O$ and at 40 °C at the tetrahydrate (5.63 mol $NiCl_2$/kg H_2O).[50] At both temperatures in dilute nickel(II) chloride solutions (≤2.0 *m*) $Ni(OH)_2$ represents the solid phase. The solubility of nickel(II) hydroxide rises with increasing concentration of nickel(II) chloride. In high concentrated nickel(II) chloride solutions a beginning conversion of $Ni(OH)_2$ into $Ni_3Cl_{2.1}(OH)_{3.9}\cdot 4H_2O$ can be observed and is accompanied by a decrease in the OH^- solution concentration. The extrapolated "OH^- line" from higher molal nickel(II) chloride solutions to 1 *m* reveals that nickel(II) hydroxide should be assumed as a metastable phase in >1 *m* nickel(II) chloride solutions because of the higher solubility (Figure 3). The incomplete conversion of $Ni(OH)_2$ in concentrated nickel(II) chloride solutions (>3.0 *m*) indicates that the system $Ni(OH)_2$−$NiCl_2$−H_2O after three months is still far away from an equilibrium state both at 25 and 40 °C.

Characterization of $Ni_3Cl_{2.1}(OH)_{3.9}\cdot 4H_2O$ in Comparison to $Mg_3Cl_2(OH)_4\cdot 4H_2O$. *Structure Description.* The main building blocks within the crystal structure of $Ni_3Cl_{2.1}(OH)_{3.9}\cdot 4H_2O$ (= $1.95Ni(OH)_2\cdot 1.05NiCl_2\cdot 4H_2O$ = 1.95−1.05−4 phase) are infinite triple chains of edge-linked NiO_6 respective NiO_5O/Cl octahedra running in [010] direction. The inner NiO_6 polyhedra show only little distortion (Table 3) and share 6 out of 12 edges with 6 different neighboring octahedra (Figure 4). All O atoms of the NiO_6 octahedra are bridging three polyhedra. The outer NiO_5O/Cl octahedra are very distorted and share only four edges with four different polyhedra. Three O atoms connect three octahedra, two O atoms connect two octahedra, and the residual O/Cl atom is a nonbridging vertex. The vertex shows an occupational disorder

Table 4. Chemical Analysis of the Solid Phase, Obtained by Precipitation Using NaOH and 4.7 *m* Nickel(II) Chloride Solution

content of Ni^{2+}	content of OH^-	content of Cl^-	content of H_2O
22.6 ± 0.2 mol % (44.7 ± 0.4 mass %)	29.5 ± 0.3 mol % (16.9 ± 0.2 mass %)	15.8 ± 0.2 mol % (18.9 ± 0.2 mass %)	32.1 ± 0.7 mol %[a] (19.5 ± 0.4 mass %) 18.9 mass%[b]
resulting composition			xNi(OH)$_2$:yNiCl$_2$:zH$_2$O ratio
$Ni_3Cl_{2.1}(OH)_{3.9}\cdot 4H_2O$			$1.95Ni(OH)_2$:$1.05NiCl_2$:$4H_2O$

[a]Calculated out of the mass balance. [b]Result of thermal analysis (see below).

dx.doi.org/10.1021/ic500251x | Inorg. Chem. 2014, 53, 4316−4324

Table 5. Composition of the Liquid Phase in the System $Ni(OH)_2$–$NiCl_2$–H_2O and the Corresponding Solid Phases at 25°C and 40°C after Three Months

no.	m $NiCl_2$ [mol/kg H_2O]	10^2 · m $Ni(OH)_2$ [mol/kg H_2O]	solid phase
		25 °C	
1	0.29	0.04	$Ni(OH)_2$
2	0.49	0.09	$Ni(OH)_2$
3	0.98	0.42	$Ni(OH)_2$
4	1.47	1.32	$Ni(OH)_2$
5	1.96	2.61	$Ni(OH)_2$
6	3.32	1.45	$Ni(OH)_2$ + $Ni_3Cl_{2.1}(OH)_{3.9}·4H_2O$
7	4.30	2.25	$Ni(OH)_2$ + $Ni_3Cl_{2.1}(OH)_{3.9}·4H_2O$
		40 °C	
8	0.28	0.06	$Ni(OH)_2$
9	0.48	0.09	$Ni(OH)_2$
10	0.96	0.43	$Ni(OH)_2$
11	1.43	1.15	$Ni(OH)_2$
12	1.97	2.01	$Ni(OH)_2$
13	3.13	0.60	$Ni(OH)_2$ + $Ni_3Cl_{2.1}(OH)_{3.9}·4H_2O$
14	4.53	0.74	$Ni(OH)_2$ + $Ni_3Cl_{2.1}(OH)_{3.9}·4H_2O$

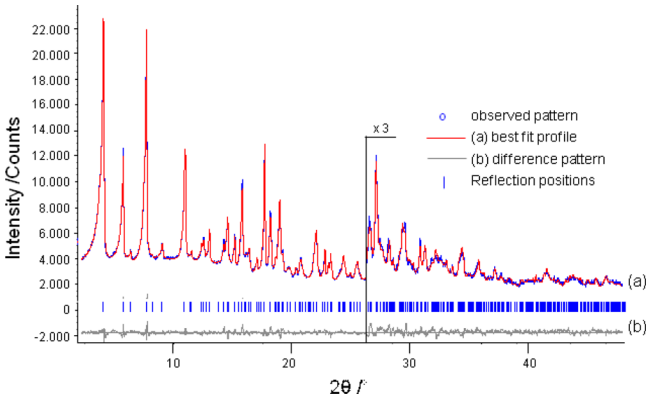

Figure 1. Scattered X-ray intensities of $Ni_3Cl_{2.1}(OH)_{3.9}·4H_2O$ at ambient conditions as a function of diffraction angle 2θ. The observed pattern (circles) measured in Debye–Scherrer geometry, the best Rietveld fit profiles (line), and the difference curve between the observed and the calculated profiles (below) are shown. The high-angle part starting at 27.0° 2θ is enlarged for clarity.

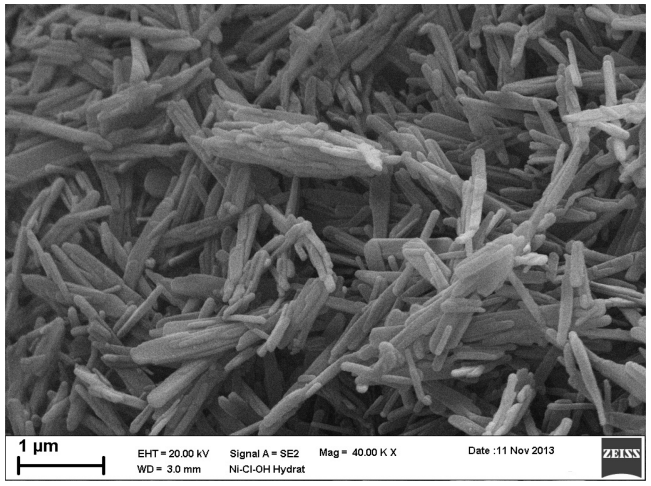

Figure 2. SEM photo of $Ni_3Cl_{2.1}(OH)_{3.9}·4H_2O$ after removal of the mother liquor and desiccation.

of O and Cl atoms. This site is occupied by O and Cl in an almost 1:1 ratio (Table 2).

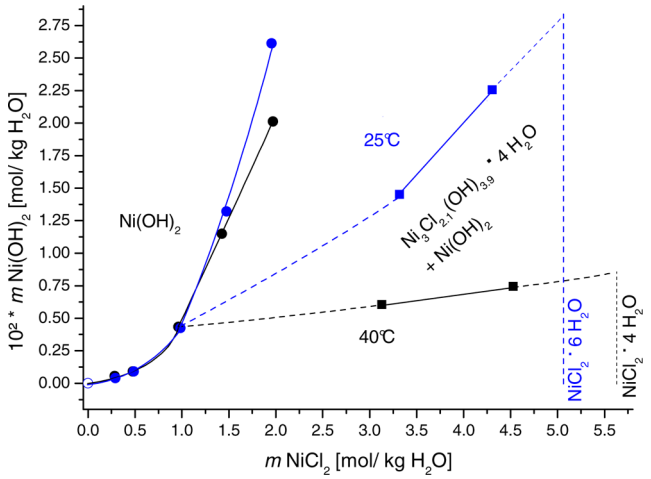

Figure 3. Composition of the liquid phase relating to the solid phases in the system $Ni(OH)_2$–$NiCl_2$–H_2O at 25 °C (blue) and 40 °C (black) after three months.

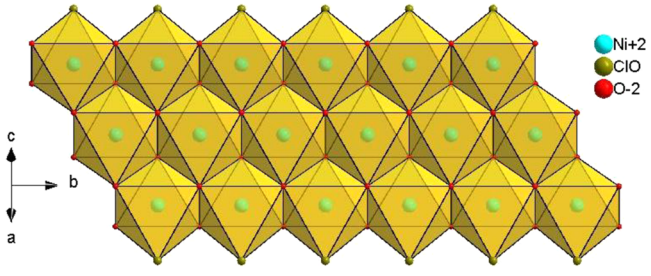

Figure 4. Sheets of infinite triple chains of Ni coordination polyhedra in [302] direction the crystal structure of $Ni_3Cl_{2.1}(OH)_{3.9}·4H_2O$.

The structure of $Ni_3Cl_{2.1}(OH)_{3.9}·4H_2O$ is closely related to the brucite-type structure of β-$Ni(OH)_2$.[30] In both structures Ni is coordinated by six ligands in an octahedral way. The octahedra are edge-linked and form definite layers (Figure 5). In the nickel hydroxide structure there are only hydroxide ions within the coordination sphere of nickel, and the layers are stacked in [001] direction in an AA-type (Figure 5 top). However, in the structure of $Ni_3Cl_{2.1}(OH)_{3.9}·4H_2O$, two oxygen sites are replaced by occupational disordered chloride

dx.doi.org/10.1021/ic500251x | Inorg. Chem. 2014, 53, 4316–4324

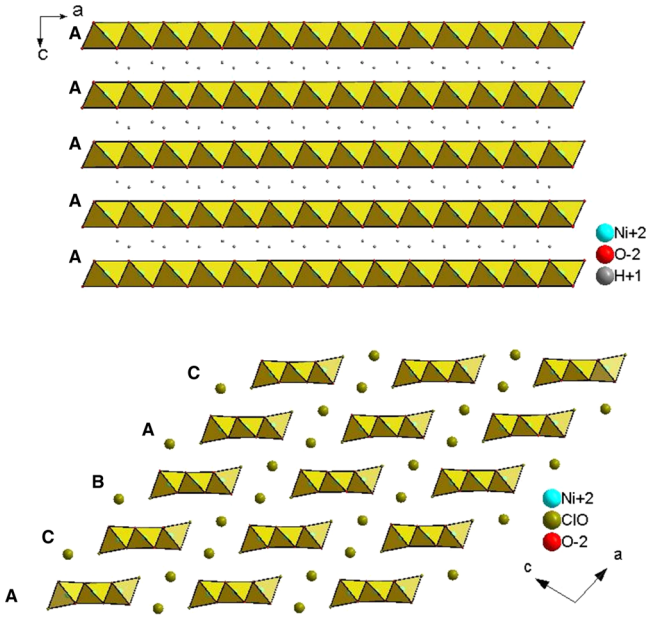

Figure 5. Stacking of β $Ni(OH)_2$[30] (top, stacking in [001] direction, viewed in [010] direction) and $Ni_3Cl_{2.1}(OH)_{3.9}\cdot 4H_2O$ (bottom, stacking in [101] direction, viewed in [010] direction).

and hydroxide ions, water molecules, which yield in a distortion of the terminal NiO_5O/Cl octahedra because of the larger ionic radius of chloride. Moreover, the triple chains of $Ni_3Cl_{2.1}(OH)_{3.9}\cdot 4H_2O$ are stacked in [101] direction in an ABC-cubic-type (Figure 5, bottom). These layers are intercepted by an interstitial zigzag chain of disordered Cl^- ions and water molecules. Because of the small distance (2.879 Å) between interstitial Cl^-/H_2O (Cl5/O5, Table 2) and both the neighboring and the subjacent terminal NiO_5O/Cl octahedra (O1, Table 2), it is supposed that the attractive interaction of the interstitial Cl^-/H_2O and these two triple chains causes the ABC-type stacking of $Ni_3Cl_{2.1}(OH)_{3.9}\cdot 4H_2O$. The interstitial Cl^-/H_2O indicate that two of five cation positions within the layers of the basic nickel chloride hydrate are vacant, whereas all anion positions are occupied by Cl^-, OH^-, or H_2O (Figure 6, bottom). If all hydroxide ion positions remain unaltered there is an excess of four negative charges. Consequently, exactly four uncharged molecules (water) occupy these four hydroxide ions sites, and the charge balance is kept. From this structural point of view, the nickel chloride

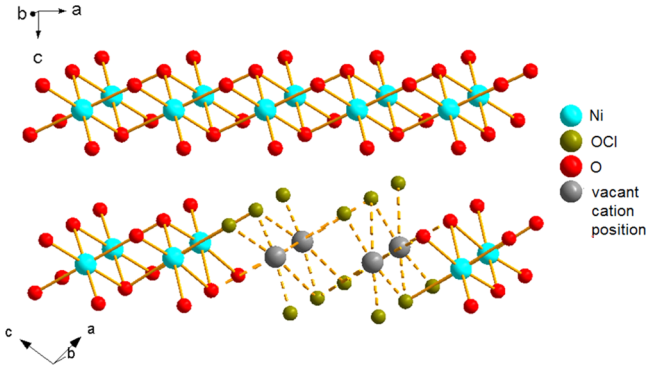

Figure 6. Excerpt of β $Ni(OH)_2$ layer (top), excerpt of a layer of $Ni_3Cl_{2.1}(OH)_{3.9}\cdot 4H_2O$ (bottom) including the illustration of vacancies (gray) within the cation lattice.

hydroxide phase has to contain exactly four molecules of crystal water, and with respect to the vacant cation positions the formula could also be written as $Ni_3\square_2Cl_{2.1}(OH)_{3.9}\cdot 4H_2O$. As there is no obvious limitation in the occupancies of those sites, the phase stochiometry might be variable and could depend on the formation conditions of the phase. In this respect, $Ni_3Cl_{2.1}(OH)_{3.9}\cdot 4H_2O$ could be a member of a phase series $Ni_3Y_2Cl_{2+x}(OH)_{4-x}\cdot 4H_2O$ around the "ideal" $Ni_3Cl_2(OH)_4\cdot 4H_2O$ (2−1−4) stoichiometry.

Another important fact is that both the crystal structures and compositions of $Ni_3Cl_{2.1}(OH)_{3.9}\cdot 4H_2O$ and $Mg_3Cl_2(OH)_4\cdot 4H_2O$ (= $2Mg(OH)_2\cdot 1MgCl_2\cdot 4H_2O$ = 2−1−4 phase)[27] are almost equal (Figure 7). So the phases can be considered as

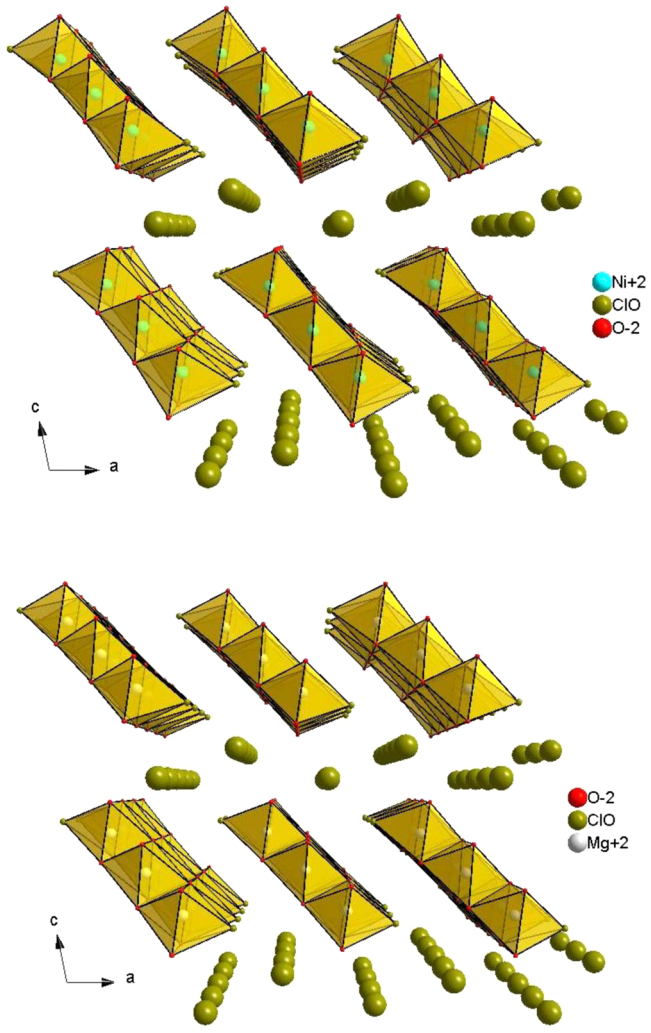

Figure 7. Packing diagrams of $Ni_3Cl_{2.1}(OH)_{3.9}\cdot 4H_2O$ (top) and $Mg_3Cl_2(OH)_4\cdot 4H_2O$[27] (bottom) viewed in [0−10] direction.

isostructural compounds. Because of the larger ionic radius of magnesium (Mg^{2+}: 0.86 Å;[29] Ni^{2+}: 0.83 Å[29]) both the lattice parameters of the 2−1−4 phase and most of the metal-anion distances are enlarged in comparison to $Ni_3Cl_{2.1}(OH)_{3.9}\cdot 4H_2O$ (Table 6). Hence the peaks in the powder pattern of $Mg_3Cl_2(OH)_4\cdot 4H_2O$ are shifted toward smaller values of 2θ. Besides this fact, the powder patterns of $Ni_3Cl_{2.1}(OH)_{3.9}\cdot 4H_2O$ and the related Mg phase are almost identical (Supporting Information, Figure 12).

dx.doi.org/10.1021/ic500251x | Inorg. Chem. 2014, 53, 4316−4324

Table 6. Comparison of Structural Data and Positions of OH-Stretching Vibration Bands of β-$Ni(OH)_2$, β-$Mg(OH)_2$, $Mg_3Cl_2(OH)_4{\cdot}4H_2O$, and $Ni_3Cl_{2.1}(OH)_{3.9}{\cdot}4H_2O$)

Compound	**β-Ni(OH)$_2$**[30]		**β-Mg(OH)$_2$**[30]	
Space group	*P*-3*m*1 (164)		*P*-3*m*1 (164)	
a **/Å**	3.1286(1)		3.1486(1)	
c **/Å**	4.6060(1)		4.7713(1)	
Atoms	**distance /Å**	$\overline{\upsilon_{OH}}$ **/ cm^{-1}**	**distance /Å**	$\overline{\upsilon_{OH}}$**/ cm^{-1}**
M(1)-O(1)	2.0595(9)	3635[46]	2.1010(10)	3698[46]
Compound	**$Ni_3Cl_{2.1}(OH)_{3.9}\cdot 4\ H_2O$**		**$Mg_3Cl_2(OH)_4\cdot 4\ H_2O$**[27]	
Space group	*C*2/*m* (12)		*C*2/*m* (12)	
a **/Å**	14.9575(4)		15.1263(3)	
b **/Å**	3.1413(1)		3.1707(1)	
c **/Å**	10.4818(5)		10.5236(2)	
β **/°**	101.482(1)		101.546(2)	
Atoms	**distance /Å**	$\overline{\upsilon(OH)}$ **/ cm^{-1}**	**distance /Å**[27]	$\overline{\upsilon(OH)}$ **/ cm^{-1}**
M1-O4/Cl4	2.324(6)	3515	2.374(7)	3568
M1-O1	2.239(6)	3582	2,240(4)	3671
M1-O2	2.046(9)	} 3611	2.098(7)	} 3644
M2-O2	2.103(6)		2.157(6)	
M1-O3	2.030(6)	} 3622	2.057(4)	} 3654
M2-O3	2.095(10)		2.153(3)	

IR Spectra. The structural similarity of $Ni_3Cl_{2.1}(OH)_{3.9}{\cdot}4H_2O$ and $Mg_3Cl_2(OH)_4{\cdot}4H_2O$ leads to comparable IR spectra. In the region of OH^- stretching vibrations (2500−3800 cm^{-1}) there are at least four very broad bands, referring to crystal water, and four sharps bands, referring to hydroxide ions, which are similar in the spectra of both compounds (Figure 8, Table

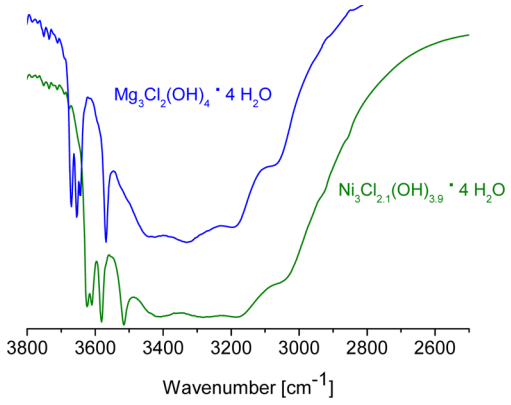

Figure 8. IR spectra of $Mg_3Cl_2(OH)_4{\cdot}4H_2O$ (top) and $Ni_3Cl_{2.1}(OH)_{3.9}{\cdot}4H_2O$ (bottom) in the region of 3800−2500 cm^{-1}.

6, Supporting Information Table 8). Three of the OH^- vibration bands are close to each other (3644−3671 cm^{-1} for Mg phase and 3582−3622 cm^{-1} for the Ni phase), and the remaining band (3568 cm^{-1} for the Mg phase and 3515 cm^{-1} for the Ni phase) is isolated. In both crystal structures there are five crystallographically distinct oxygen sites (Figure 10). Since there are only four OH^- stretching vibrations, one site must be exclusively occupied by water. All OH^- stretching bands are shifted from $Mg_3Cl_2(OH)_4{\cdot}4H_2O$ to $Ni_3Cl_{2.1}(OH)_{3.9}{\cdot}4H_2O$ at about 32 to 89 cm^{-1} toward lower wavenumbers, due to the higher covalent part of the metal−oxygen bond of the nickel phase, which softens the H−O bond, causing a downshift of the OH^- stretching vibration.[50−53] Thus, every hydroxide ion has to be located within the coordination sphere of a metal ion. Hence the interstitial, occupationally disordered site O5/Cl5 is

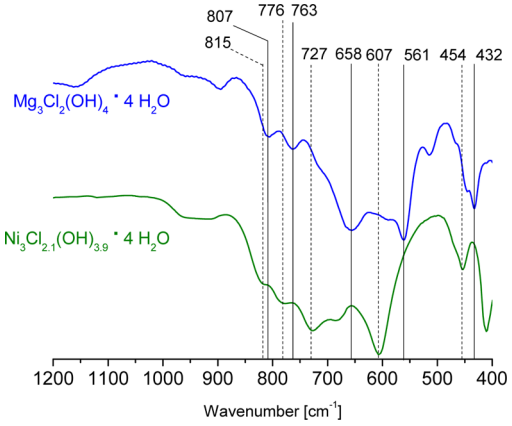

Figure 9. Infrared spectra of $Mg_3Cl_2(OH)_4{\cdot}4H_2O$ (top) and $Ni_3Cl_{2.1}(OH)_{3.9}{\cdot}4H_2O$ (bottom) in the region of 1200−400 cm^{-1}.

occupied by a chloride ion or a water molecule. All other oxygen positions might show an occupational disorder of water and hydroxide, since water must also occupy oxygen positions besides O5/Cl5 with regard to phase stoichiometry. Because of the correlation of metal−oxide bond lengths with OH stretching frequencies,[50,53] the isolated OH^- stretching band must refer to the site O4/Cl4 due to the longest metal−oxygen distance and to the nonbridging vertex position. Both sites O2 and O3 are coordinated by three metal ions, and the corresponding metal−oxygen distances show only slight differences (Figure 10 and Table 6). Thus, the OH^- vibration bands almost overlapping (3644 and 3654 cm^{-1} and 3611 and 3622 cm^{-1}) must refer to the hydroxide ions situated on these sites. The downshift of the OH^- band of O1 from the magnesium phase (3671 cm^{-1}) to the nickel phase (3582 cm^{-1}) is immense and cannot be explained by the transition-metal effect only. There is a slight difference in the crystal structures of $Ni_3Cl_{2.1}(OH)_{3.9}{\cdot}4H_2O$ and $Mg_3Cl_2(OH)_4{\cdot}4H_2O$. Because of the smaller ionic radius of Ni^{2+} nearly all nickel−oxygen distances are clearly shorter than the magnesium−oxygen ones. But the bond Ni1−O1 is almost as long as the

dx.doi.org/10.1021/ic500251x | Inorg. Chem. 2014, 53, 4316−4324

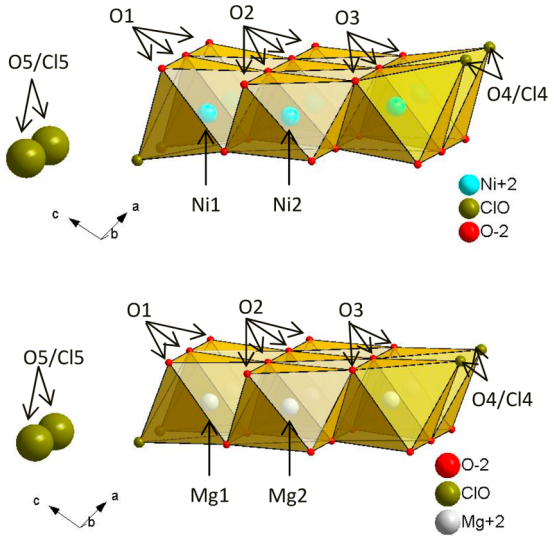

Figure 10. Atom sites in polyhedra of $Ni_3Cl_{2.1}(OH)_{3.9}·4H_2O$ (top) and $Mg_3Cl_2(OH)_4·4H_2O$ (bottom) in correlation to the IR data in Table 3.

one of the corresponding atoms in the magnesium phase. The correlation of metal−oxide bond lengths with OH stretching frequencies[50,53] explains best of all the enormous downshift of the corresponding OH^- stretching vibration.

The IR spectra of $Ni_3Cl_{2.1}(OH)_{3.9}·4H_2O$ and $Mg_3Cl_2(OH)_4·4H_2O$ in the region of the M−O and H−O−H deformation bands (400 to 1500 cm^{-1}) are given in Figure 9. There are many broad overlapping bands, and both IR spectra are similar in the region of lattice vibrations (Supporting Information, Table 8). These vibrations are mainly caused by M−O stretching vibrations of the MO_6 and MO_5O/Cl octahedra. There is a slight upshift of the wavenumbers of the lattice vibrations from the Mg phase to the Ni phase. As the $M(O2)_4(O3)_2$ octahedra are similar to the MO_6 ones in the corresponding hydroxides, the M−O stretching band at 454 cm^{-1} (Ni phase) and 432 cm^{-1} (Mg phase) is also quite similar to the M−O band of the hydroxides (449 cm^{-1} for $Ni(OH)_2$ and 443 cm^{-1} for $Mg(OH)_2$).[54] Slight differences may be caused by the small influence of interstitial chloride and water, by the occupational disorder of water and hydroxide, and by the slight distortion of the MO_6 octahedra in the basic metal(II) chloride hydrates.

Thermal Behavior. Dehydration of $Ni_3Cl_{2.1}(OH)_{3.9}·4H_2O$ occurs in a three-step process, which starts at about 85 °C. The first step overlaps with the second one, and both steps correlate with sharp endothermic effects. At approximately 180 °C the last step of dehydration begins, which correlates with a very broad endothermic effect. At 250−270 °C the release of crystal water is completed with a mass loss of 18.9%, corresponding to 4.09 mol of water (theoretical = 18.5% for four water molecules, Table 7). The measuring conditions (heating rate = 2 K min^{-1}) used for $Ni_3Cl_{2.1}(OH)_{3.9}·4H_2O$ were also applied to a sample of $Mg_3Cl_2(OH)_4·4H_2O$ (the compound was still available from our earlier investigation[27]). Accordingly, the dehydration process of the magnesium phase also occurs in three steps. The initial temperatures of these steps are higher than those for $Ni_3Cl_{2.1}(OH)_{3.9}·4H_2O$, which could be caused by the low crystallinity of the Ni phase (Figure 1) and/or a higher affinity of magnesium to the coordinating water oxygen.

After a plateau the dehydration of the hydroxide ions of the nickel compound begins at 300−320 °C and takes place in two steps. At first structural water is released, which correlates with a sharp endothermic effect. X-ray powder diffraction showed that the residue contains exclusively NiO and $NiCl_2$ (Supporting Information, Figure 13); the latter undergoes a slow and complete hydrolysis, caused by traces of water in the argon flow, yielding to NiO as the only solid phase, which is present in the residue of the thermal decomposition, confirmed by X-ray powder diffraction. During the total thermal decomposition of $Ni_3Cl_{2.1}(OH)_{3.9}·4H_2O$ into 3 mol of NiO a mass loss of 42.3% was observed (theoretically 42.4%, Table 7). The magnesium phase ($Mg_3Cl_2(OH)_4·4H_2O$) finally decomposes to the oxide, too. The thermal analyses of both phases are shown in Figure 11.

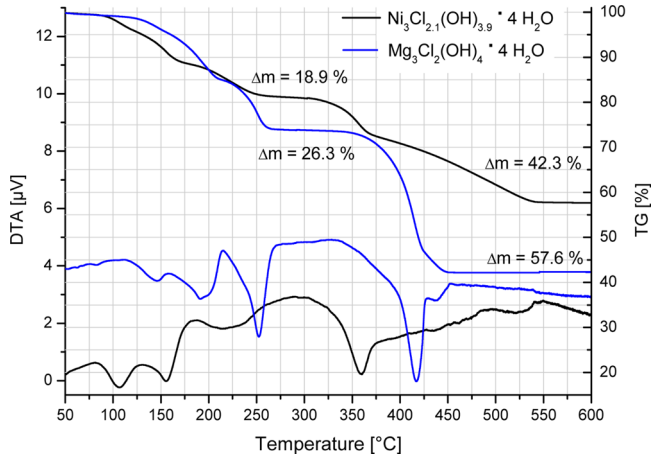

Figure 11. TG/DTA analysis curves of $Ni_3Cl_{2.1}(OH)_{3.9}·4H_2O$ and $Mg_3Cl_2(OH)_4·4H_2O$.

Final Discussion. The fact that the Ni phase $Ni_3Cl_{2.1}(OH)_{3.9}·4H_2O$ is found to be isostructural to $Mg_3Cl_{2.0}(OH)_{4.0}·4H_2O$ is quite surprising, as this Ni phase is the first known basic transition-metal hydrate that is isostructural to a Mg-hydrate phase. All known naturally occurring basic divalent transition-metal chloride hydrates, such as Claringbullite ($Cu_4Cl(Cl_{0.29}OH_{0.71})(OH)_6$),[55] Bobkingite ($Cu_5(OH)_8Cl_2·2H_2O$),[56] Simoncolleite ($Zn_5(OH)_8Cl_2·$

Table 7. Mass Loss during the Thermal Decomposition of $Ni_3Cl_{2.1}(OH)_{3.9}·4H_2O$

temp. range, °C	thermal effect	total $\Delta m_{(theoretical)}$	total $\Delta m_{(measured)}$	reaction according to total mass lost
85−180	endotherm, middle	9.3%	10.4%	$Ni_3Cl_{2.1}(OH)_{3.9}·4H_2O \rightarrow Ni_3Cl_{2.1}(OH)_{3.9}·2H_2O + 2H_2O$
180−270	endotherm, broad	18.5%	18.9%	$Ni_3Cl_{2.1}(OH)_{3.9}·2H_2O \rightarrow Ni_3Cl_{2.1}(OH)_{3.9} + 2H_2O$
300−370	endotherm, sharp	27.5%	27.2%	$Ni_3Cl_{2.1}(OH)_{3.9} \rightarrow 1.95NiO + 1.05NiCl_2 + 1.95H_2O$
370−550	endotherm, very broad	42.4%	42.3%	$1.95NiO + 1.05NiCl_2 + 1.05H_2O_{(g)} \rightarrow 3NiO + 2.1HCl\uparrow$

dx.doi.org/10.1021/ic500251x | Inorg. Chem. 2014, 53, 4316−4324

H_2O),[57] or synthesized basic divalent transition-metal chloride hydrates like $Co_{1.176}(OH)_2Cl_{0.384}\cdot 0.456H_2O$ (α-$Co(OH)_2$)[58] show vast differences both in the composition of the phases and in crystal structure constitution to basic magnesium chloride (hydrates) phases. As Ni^{2+} is a d^8 cation, it tends toward a Jahn–Teller-like distorted octahedral coordination, especially if there are two different types of ligands available, that may enter the coordination sphere as in $NiCl_2\cdot 6H_2O$.[34] Mg^{2+}, a main-group metal cation, tends toward a regular octahedral coordination, as in $MgCl_2\cdot 6H_2O$.[33] From this structural point of view the existence of isostructural basic nickel and magnesium chloride hydrates was not to be expected.

CONCLUSIONS

The formation of crystalline, basic nickel(II) chloride phases at ambient temperatures is observed as a very slow process. A systematic search for phases in the system of $Ni(OH)_2$–$NiCl_2$–H_2O at 25 and 40 °C for three months resulted in only one crystalline hydrate phase with the composition of $Ni_3Cl_{2.1}(OH)_{3.9}\cdot 4H_2O$ [= $1.95Ni(OH)_2\cdot 1.05NiCl_2\cdot 4H_2O$] beside $Ni(OH)_2$. For a detailed characterization it was possible to prepare the hydrate as a pure phase by precipitation in concentrated nickel(II) chloride solution using sodium hydroxide and subsequent crystallization in appropriate solution at 40 °C. The composition was determined by chemical analysis (volumetric methods) before the crystal structure of $Ni_3Cl_{2.1}(OH)_{3.9}\cdot 4H_2O$ was solved and refined from high-resolution X-ray laboratory powder diffraction data employing the methods of global optimization and Rietveld refinement. Because of structural considerations the phase composition is supposed to be variable in terms of the $Ni(OH)_2/NiCl_2$ ratio according to the formula of $Ni_3Cl_{2+x}(OH)_{4-x}\cdot 4H_2O$. The basic magnesium chloride hydrate, $Mg_3Cl_2(OH)_3\cdot 4H_2O$ (2–1–4 phase) was found to be isostructural to $Ni_3Cl_{2.1}(OH)_{3.9}\cdot 4H_2O$, showing also a similar thermal behavior, thus confirming $Ni_3Cl_{2.1}(OH)_{3.9}\cdot 4H_2O$ as the Ni analogue of $Mg_3Cl_2(OH)_3\cdot 4H_2O$ (2–1–4 phase). Slight structural differences correspond to the shifts of OH-stretching vibrations in the IR spectra.

ASSOCIATED CONTENT

Supporting Information

This features X-ray powder diffraction patterns, tabluated IR data, and TG/DTA data. This material is available free of charge via the Internet at http://pubs.acs.org.

AUTHOR INFORMATION

Corresponding Author

*E-mail: daniela.freyer@chemie.tu-freiberg.de (D.F.).

Notes

The authors declare no competing financial interest.

REFERENCES

(1) Sorel, S.; Dumas, M. *C. R. Acad. Sci., Paris* **1867**, *65*, 102–104.
(2) Feitknecht, W. *Helv. Chim. Acta* **1926**, *9*, 1018–1049.
(3) Feitknecht, W.; Held, F. *Helv. Chim. Acta* **1927**, *10*, 140–167.
(4) Feitknecht, W.; Held, F. *Helv. Chim. Acta* **1930**, *13*, 1380–1390.
(5) Feitknecht, W.; Held, F. *Helv. Chim. Acta* **1944**, *27*, 1480–1495.
(6) Feitknecht, W.; Oswald, H. R. *Helv. Chim. Acta* **1964**, *47*, 272–289.
(7) Lukens, H. S. *J. Am. Ceram. Soc.* **1932**, *54*, 2372–2380.
(8) Bury, C. R.; Davies, E. R. H. *J. Chem. Soc.* **1932**, 2008–2015.
(9) Walter-Levy, L.; de Wolff, P. M. *C. R. Acad. Sci., Paris* **1949**, *229*, 1077–1079.
(10) Walter-Levy, L.; de Wolff, P. M. *C. R. Acad. Sci., Paris* **1949**, *229*, 1232–1234.
(11) Walter-Levy, L.; Bianco, Y. *C. R. Acad. Sci., Paris* **1951**, *232*, 730–732.
(12) Bianco, Y. *C. R. Acad. Sci., Paris* **1951**, *232*, 1108–1110.
(13) Cole, W. F.; Demediuk, T. *Aust. J. Chem.* **1955**, *8* (2), 234–251.
(14) Demediuk, T.; Cole, W. F.; Hueber, H. V. *Aust. J. Chem.* **1955**, *8*, 215–233.
(15) D'Ans, J.; Busse, W.; Freund, H.-E. *Kali Steinsalz* **1955**, *8*, 3–7.
(16) Bianco, Y. *Ann. Chim. (Paris, Fr.)* **1958**, *3*, 370–405.
(17) Ball, M. *Cem. Concr. Res.* **1977**, *7*, 575–584.
(18) Xia, S.; Xing, P.; Gao, S. *Thermochim. Acta* **1991**, *183*, 349–363.
(19) Kanesaka, I.; Aoyama, S. *J. Raman Spectrosc.* **2001**, *32*, 361–367.
(20) Kanesaka, I.; Shimizu, R. *Spectrochim. Acta* **2003**, *A 59*, 569–573.
(21) Altmaier, M.; Metz, V.; Neck, V.; Müller, R.; Fanghänel, T. *Geochim. Cosmochim. Acta* **2003**, *67* (19), 3595–3601.
(22) Xiong, Y.; Deng, H.; Nemer, M.; Johnsen, S. *Geochim. Cosmochim. Acta* **2010**, *74*, 4605–4611.
(23) Dinnebier, R. E.; Halasz, I.; Freyer, D.; Hanson, J. C. *Z. Anorg. Allg. Chem.* **2011**, *637* (11), 1458–1462.
(24) de Wolff, P. M.; Walter-Levy, L. *Acta Crystallogr. (1,1948–23,1967)* **1953**, *6*, 40–44.
(25) Sugimoto, K.; Dinnebier, R. E.; Schlecht, T. *Acta. Crystallogr., Sect. B* **2007**, *63*, 805–811.
(26) Dinnebier, R. E.; Freyer, D.; Bette, S.; Oestreich, M. *Inorg. Chem.* **2010**, *49*, 9770–9776.
(27) Dinnebier, R. E.; Oestreich, M.; Bette, S.; Freyer, D. *Z. Anorg. Allg. Chem.* **2012**, *638*, 628–633.
(28) de Wolff, P. M.; Kortlandt, D. *Appl. Sci. Res., Sect. B* **1954**, *3*, 400–408.
(29) Shannon, R. D. *Acta Crystallogr.* **1976**, *A32*, 751–767.
(30) Kazimirov, V. Y.; Smirnov, M. B.; Bourgeois, L.; Guerlou Demourgues, L.; Servant, L.; Balagurov, A. M.; Natkaniec, I.; Khasanova, N. R.; Antipov, E. V. *Solid State Ionics* **2010**, *181*, 1764–1770.
(31) Sugimoto, K.; Dinnebier, R. E.; Hanson, J. C. *Acta. Crystallogr., Sect. B* **2007**, *63*, 235–242.
(32) Schmidt, H.; Hennings, E.; Voigt, W. *Acta. Crystallogr., Sect. C: Cryst. Struct. Commun.* **2012**, *68*, 4–6.
(33) Agron, P. A.; Busing, W. R. *Acta. Crystallogr., Sect. A* **1969**, *25*, 118–119.
(34) Kleinberg, R. *J. Chem. Phys.* **1969**, *50*, 4690–4696.
(35) Waizumi, K.; Masuda, H.; Ohtaki, H. *Inorg. Chem. Acta* **1992**, *192*, 173–181.
(36) Morosin, B. *Acta Crystallogr. (11,948–23,1967)* **1967**, *23*, 630–634.
(37) Vilminot, S.; Richard-Plouet, M.; André, G.; Swierczynski, D.; Bourée-Vigneron, F.; Kurmoo, M. *Inorg. Chem.* **2003**, *42*, 6859–6867.
(38) Feitknecht, W.; Collet, A. *Helv. Chim. Acta* **1939**, *22*, 1428–1444.
(39) Makovskaya, G. V.; Spivakovskii, V. B. *Zh. Neorg. Khim.* **1969**, *14*, 1478–1483.
(40) André, G. *C. R. Acad. Sci., Paris* **1888**, *106*, 936–939.
(41) Gire, G.; de Narbonne, A. M. *C. R. Acad. Sci., Paris* **1934**, *198*, 2250–2252.
(42) Kamath, P. V.; Therese, G. H. A.; Gopalakrishnan, J. *J. Solid State Chem.* **1997**, *128*, 38–41.
(43) Pannach, M.; Freyer, D.; Altmaier, M.; Bube, C.; Metz, V.; Voigt, W. *Geochim. Cosmochim. Acta* submitted for publication.
(44) *Topas,* version 4.2; Bruker AXS: Karlsruhe, Germany, 2009.
(45) Coelho, A. A. *J. Appl. Crystallogr.* **2003**, *36*, 86–95.
(46) LeBail, A.; Duroy, H.; Fourquet, J. L. *Mater. Res. Bull.* **1988**, *23*, 447–452.
(47) Cheary, R. W.; Coelho, A. A.; Cline, J. P. *J. Res. Natl. Inst. Stand. Technol.* **2005**, *109*, 1–25.
(48) Coelho, A. A. *J. Appl. Crystallogr.* **2000**, *33*, 899–908.

(49) Brindley, G. W.; Kao, C. C. *Phys. Chem. Miner.* **1984**, *10*, 187−191.
(50) Boye, E. *Z. Anorg. Allg. Chem.* **1933**, *216*, 29−32.
(51) Lutz, H. D.; Henning, J.; Haeuseler, H. *J. Mol. Struct.* **1987**, *156*, 143−145.
(52) Beckenkamp, K.; Lutz, H. D. *J. Mol. Struct.* **1992**, *270*, 393−405.
(53) de Oliveira, E. F.; Hase, Y. *Vib. Spectrosc.* **2003**, *31*, 19−24.
(54) Lutz, H. D.; Möller, H.; Schmidt, M. *J. Mol. Struct.* **1994**, *328*, 121−132.
(55) Burns, P. C.; Cooper, M. A.; Hawthrone, F. C. *Can. Mineral.* **1995**, *33*, 633−639.
(56) Hawthorne, F. C.; Cooper, M. A.; Grice, J. D.; Roberts, A. C.; Hubbard, N. *Mineral. Mag.* **2002**, *66*, 301−311.
(57) Hawthorne, F. C.; Sokolova, E. *Can. Mineral.* **2002**, *40*, 939−946.
(58) Renzhi, M.; Liu, Z.; Takada, K.; Fukuda, K.; Ebina, Y.; Bando, Y.; Sasaki, T. *Inorg. Chem.* **2006**, *45*, 3964−3969.

dx.doi.org/10.1021/ic500251x | *Inorg. Chem.* 2014, 53, 4316−4324